



UNIVERSITY
OF TRENTO

DIPARTIMENTO DI INGEGNERIA E SCIENZA DELL'INFORMAZIONE

38123 Povo – Trento (Italy), Via Sommarive 14
<http://www.disi.unitn.it>

HANDLING SIDEBAND RADIATIONS IN TIME-MODULATED
ARRAYS THROUGH PARTICLE SWARM OPTIMIZATION

L. Poli, P. Rocca, L. Manica, and A. Massa

January 2011

Technical Report # DISI-11-024

Handling Sideband Radiations in Time-Modulated Arrays through Particle Swarm Optimization

L. Poli, P. Rocca, L. Manica, and A. Massa

ELEDIA Research Group

Department of Information Engineering and Computer Science,

University of Trento, Via Sommarive 14, 38050 Trento - Italy

Tel. +39 0461 882057, Fax +39 0461 882093

E-mail: *andrea.massa@ing.unitn.it*,

{lorenzo.poli, paolo.rocca, luca.manica}@disi.unitn.it

Web-site: *http://www.eledia.ing.unitn.it*

Handling Sideband Radiations in Time-Modulated Arrays through Particle Swarm Optimization

L. Poli, P. Rocca, L. Manica, and A. Massa

Abstract

In this letter, the minimization of the power losses in time-modulated arrays is addressed by means of a suitable strategy based on Particle Swarm Optimization. By properly modifying the modulation sequence, the method is aimed at reducing the amount of wasted power, analytically computed through a very effective closed-form relationship, while constraining the radiation pattern at the carrier frequency below a fixed sidelobe level. Representative results are reported and compared with previously published solutions to assess the effectiveness of the proposed approach.

Key words: Linear Arrays, Time-Modulated Arrays, Pattern Synthesis.

1 Introduction

The use of time as an additional degree of freedom in array synthesis has been investigated in the pioneering work by Shanks and Bickmore [1]. Kummer *et al.* in [2] discussed the possibility of using *RF* switches for modulating in time the element excitations in order to obtain average low and ultra-low side lobes. Successively, only a few works (e.g., [3]) have dealt with time modulation. As pointed out in [2][4], the main difficulties to the diffusion of such a technique lie in its technical implementation. However, some recent prototypes [5][6] and new interesting applications (e.g., the synthesis of sum and difference patterns [7] or the realization of phase switched screens [6]) have renewed the interest on time-modulated arrays as well as on its practical feasibility.

By a theoretical point of view, the modulation of the array excitations with *RF* switches generates undesired harmonic radiations and power losses. In order to reduce sideband radiations (*SRs*), different stochastic iterative algorithms have been proposed [5][8][9][10]. They are based on the minimization of the sideband levels (*SBLs*) at the higher order harmonics. However, such a guideline presents some disadvantages. First, it enforces an “indirect” *SRs* reduction (i.e., through *SBLs* minimization). Moreover, it needs the computation of the *SBL* at each harmonic frequency. As a matter of fact, neglecting some higher harmonics and considering just low orders could prevent a suitable *SR* reduction. In order to overcome these drawbacks, this paper presents an innovative approach based on a Particle Swarm Optimizer (*PSO*) [11] aimed at synthesizing a desired pattern with a prescribed sidelobe level (*SLL*) at the carrier frequency also directly minimizing the power losses due to *SRs*. Towards this end, the closed-form relationship, derived in [4] to quantify the total power wasted in sideband radiations, is profitably exploited because of its analytic form, its simplicity, and to avoid the evaluation of the (infinite) set of higher harmonic patterns.

The outline of the paper is as follows. In Sect. 2, the key-issues concerned with time-modulation for the array synthesis are briefly summarized. Successively, the *PSO*-based strategy for the reduction of the power losses due to *SRs* is described. Section 3 is devoted to the numerical analysis. Preliminary results are reported and compared with state-of-the-art solutions to point out the effectiveness of the proposed approach. Finally, some conclusions are drawn (Sect. 4).

2 Mathematical Formulation

Let us consider a time-modulated linear array of N (without loss of generality) isotropic elements located at $z_n = nd$, $n = 0, \dots, N - 1$, (d being the inter-element distance) along the z axis. The corresponding array factor is given by [2]

$$F(\theta, t) = e^{j\omega_0 t} \sum_{n=0}^{N-1} I_n(t) e^{jnu} \quad (1)$$

where $\omega_0 = 2\pi f_0$ is the carrier angular frequency, $u = \frac{\omega_0}{c} d \cos \theta$, c being the speed of light in vacuum, and θ the angle measured from the array axis. Moreover, $I_n(t) = \alpha_n U_n(t)$, $n = 0, \dots, N - 1$, are the time-modulated excitations. More specifically, $\underline{\alpha} = \{\alpha_n; n = 0, \dots, N - 1\}$ and $\underline{U}(t) = \{U_n(t); n = 0, \dots, N - 1\}$ are the set of static excitations and time-step functions of the RF switches, respectively.

Because of the periodicity of the pulse sequences, $U_n(t) = U_n(t + iT_p)$, $n = 0, \dots, N - 1$, $i \in \mathbb{Z}$,

$$U_n(t) = \begin{cases} 1 & t \leq t_n \\ 0 & t_n < t \leq T_p \end{cases}, \quad (2)$$

T_p being the time period, it is possible to express $I_n(t)$ in terms of the corresponding Fourier series

$$I_n(t) = \sum_{h=-\infty}^{\infty} A_{hn} e^{jh\omega_p t} \quad (3)$$

where $\omega_p = \frac{2\pi}{T_p}$, $A_{hn} = \alpha_n a_{hn}$, and a_{hn} is the h -th harmonic coefficient of $U_n(t)$ given by

$$a_{hn} = \frac{1}{T_p} \int_0^{T_p} U_n(t) e^{-jh\omega_p t} dt. \quad (4)$$

By substituting (3) in (1), the far field pattern radiated by the array appears to be the summation of an infinite number of harmonic contributions. More specifically, the central frequency beam is given by

$$F^{(0)}(\theta, t) = e^{j\omega_0 t} \sum_{n=0}^{N-1} \alpha_n a_{0n} e^{jnu}, \quad (5)$$

while the sideband radiations turns out to be

$$F_{SR}(\theta, t) = \sum_{h=-\infty (h \neq 0)}^{\infty} F^{(h)}(\theta, t) \quad (6)$$

where $F^{(h)}(\theta, t) = \left[\sum_{n=0}^{N-1} A_{hn} e^{jnu} \right] e^{j(h\omega_p + \omega_0)t}$.

As regards to the losses due to *SRs*, they can be analytically quantified according to the following closed form [4]

$$\mathcal{P}^{SR}(\underline{\alpha}, \underline{\tau}) = \sum_{n=0}^{N-1} \{ |\alpha_n|^2 \tau_n (1 - \tau_n) \} + \sum_{m,n=0 (m \neq n)}^{N-1} \{ \Re \{ \alpha_m \alpha_n^* \} \text{sinc} [k(z_m - z_n)] (\tau_{mn} - \tau_m \tau_n) \} \quad (7)$$

where $\Re \{ \cdot \}$ and the apex * indicate the mean real part and complex conjugation, respectively. Moreover, $\underline{\tau} = \{ \tau_n; n = 0, \dots, N-1 \}$ is the set of normalized switch-on times whose n -th element is defined as $\tau_n = \frac{t_n}{T_p}$, while

$$\tau_{mn} = \begin{cases} \tau_n & \text{if } \tau_n \leq \tau_m \\ \tau_m & \text{otherwise} \end{cases} \quad (8)$$

Therefore, it turns out that the *SR* power losses can be minimized by properly setting the values of the static excitations, $\underline{\alpha}$, as well as the durations of the time pulses, $\underline{\tau}$. However, since we are interested in synthesizing antennas with a low number of control parameters, uniform and isophoric excitations (i.e., $\alpha_n = 1, n = 0, \dots, N-1$) are assumed. Only the durations of the switch-on times are then optimized by means of an iterative (k being the iteration index) *PSO*-based strategy aimed at minimizing the following cost function

$$\Psi(\underline{\tau}) = w_{SLL} \Psi^{SLL}(\underline{\tau}) + w_P \mathcal{P}_k^{SR} \quad (9)$$

The first term in (9), $\Psi^{SLL} = H [SLL^{ref} - SLL_k] \frac{|SLL^{ref} - SLL_k|^2}{|SLL^{ref}|^2}$, models a constraint on the array pattern at ω_0 and quantifies the distance between the current, SLL_k , and the desired sidelobe level, SLL^{ref} , while the latter is related to the power losses. Moreover, w_{SLL} and w_P are real weight coefficients and $H(\cdot)$ is the Heaviside step function.

As regards to the *PSO*-based minimization, the algorithm starts from randomly chosen guess values and updates at each iteration the set of S trial solutions, $\underline{\tau}_k^{(s)}$, $s = 1, \dots, S$, as well as the corresponding *PSO* velocities, $\underline{v}_k^{(s)}$, $s = 1, \dots, S$, as follows [11]

$$\begin{aligned}\underline{v}_k^{(s)} &= e\underline{v}_{k-1}^{(s)} + C_1 r_1 \left(\underline{p}_k^{(s)} - \underline{\tau}_{k-1}^{(s)} \right) + C_2 r_2 \left(\underline{g}_k - \underline{\tau}_{k-1}^{(s)} \right) \\ \underline{\tau}_k^{(s)} &= \underline{\tau}_{k-1}^{(s)} + \underline{v}_k^{(s)}, \quad s = 1, \dots, S\end{aligned}\quad (10)$$

where e (*inertial weight*), C_1 (*cognitive acceleration*), and C_2 (*social acceleration*) are the *PSO* control parameters. Moreover, r_1 and r_2 are two random variables having uniform distribution in the range $[0 : 1]$. Furthermore, $\underline{p}_k^{(s)} = \arg \left\{ \min_{q=1, \dots, k} \left[\Psi \left(\underline{\tau}_q^{(s)} \right) \right] \right\}$ and $\underline{\tau}_k^{opt} = \arg \left\{ \min_{s=1, \dots, S} \left[\Psi \left(\underline{p}_k^{(s)} \right) \right] \right\}$ are the so-called *personal best* solution and *global best* solution, respectively. The process is iterated until a convergence criterion based either on a maximum number of iterations K or the following stationary condition

$$\left| \frac{K_{window} \Psi \left(\underline{\tau}_k^{opt} \right) - \sum_{q=1}^{K_{window}} \Psi \left(\underline{\tau}_{k-q}^{opt} \right) \Psi_l^{opt}}{\Psi \left(\underline{\tau}_k^{opt} \right)} \right| \leq \eta \quad (11)$$

holds true. In (11), K_{window} and η are a fixed number of iterations and a user-defined numerical threshold, respectively.

3 Numerical Results

This section is devoted to give some indications on the effectiveness of the proposed approach in minimizing the power losses associated to the *SRs*, while synthesizing a fixed-*SLL* pattern at the carrier frequency. Towards this purpose, some representative examples are reported and discussed also in a comparative fashion. Comments on the relationship between *SR* minimization, performance (i.e., *SLL*) and complexity of the synthesized array are given, as well.

Let us consider a linear array of $N = 30$ elements equally-spaced by $d = 0.7\lambda$. The same experiment has been previously dealt with in [10] with the aim of minimizing the sideband levels (*SBLs*) at $h = 1, 2$, while keeping a desired *SLL* at $\omega = \omega_0$. In [10], the optimization has been carried out by means of a Simulated Annealing (*SA*) approach by setting $SLL^{ref} = -20$ dB

and $SBL^{ref} = -30$ dB, respectively. The synthesized solution [10] fulfills both requirements (i.e., $SLL_{SA} = -20$ dB, $SBL_{SA}^{(1)} = -30.2$ dB, and $SBL_{SA}^{(2)} = -35.1$ dB) by time-modulating only 9 elements over 30 and the power wasted in the sidelobe radiations amounts to $\mathcal{P}_{SA}^{SR} = 3.89$ % of the total input power. The directivity and the feed-network efficiency computed through the relationships in [12] are equal to $D_{SA}^T = 15.14$ dB and $\eta_{SA}^f = 0.82$, respectively.

As far as the *PSO*-based method is concerned, a swarm of $S = 10$ particles (i.e., trial solutions) has been chosen and the control parameters have been set to $w = 0.4$, $C_1 = C_2 = 2.0$, and $K = 1000$. Moreover, a uniform weighting has been assumed in (9) (i.e., $w_{SLL} = w_P = 1.0$). The numerical simulations have been run on a 3 GHz PC with 1 GB of RAM and the convergence has been reached after $K_{end} = 761$ iterations with a total and average (per iteration) CPU time equal 113.39 [sec] and 0.149 [sec], respectively. The time sequence synthesized at $k = K_{end}$ is shown in Fig. 1 while the patterns afforded at the carrier frequency [Eq. (5)] and the first two harmonic patterns [Eq. (6) - $h = 1, 2$] are shown in Fig. 2. As it can be noticed (Fig. 1), only 4 elements are time modulated (vs. 9 in [10]) and the same performances of the *SA*-based approach have been obtained neglecting the elements 1, 26, 27, and 29, which are always turned off.

As regards to the fulfillment of the synthesis constraints, Figure 3 shows the behavior of $\Psi_k^{opt} = \Psi(\mathcal{I}_k^{opt})$ and the values of the two terms in (9). As expected, the *PSO* solution widely fulfils the user constraint on the *SLL* at the convergence [i.e., $\Psi^{SLL}(K_{end}) < 10^{-6}$], when the stationary condition on the value of the cost function is reached. Concerning the *SR*, although the sideband level of the first harmonic term of the *PSO* solution is higher than that synthesized with the *SA* approach (i.e., $SBL_{PSO}^{(1)} = -28.9$ dB vs. $SBL_{SA}^{(1)} = -30.2$ dB - Fig. 4), the amount of power losses in the *SRs* turns out to be lower since $\mathcal{P}_{PSO}^{SR} = 3.57$ %. Such a result points out that a suitable strategy based on the direct minimization of the *SR*, instead of the optimization of the *SBLs* [5][8][9][10], seems to be more effective in reducing power losses. On the other hand, it should be noticed that the proposed techniques also guarantees satisfactory *SBLs* since, besides the first harmonic ($h = 1$), $SBL_{PSO}^{(h)} < SBL_{SA}^{(h)}$ for $h \geq 2$. As a matter of fact, the reduction of the *SBL* ranges from a minimum of $\Delta_{min}^{SBL} = 0.7$ dB to a maximum equal to $\Delta_{max}^{SBL} = 11.5$ dB, with an average value of around $\Delta_{av}^{SBL} = 6.2$ dB. Conversely, the directivity

as well as the feed-network efficiency slightly reduce to $D_{PSO}^T = 14.94 \text{ dB}$ and $\eta_{PSO}^f = 0.79$. Finally, Figure 5 gives some indications on the trade-off between antenna performance (i.e., directivity and SLL) and associated power losses, \mathcal{P}^{SR} , when considering Dolph-Chebyshev distributions [13]. As expected, it is worth noting that there is an inverse relationship between the amount of power losses and the maximum directivity for time-modulated linear arrays.

4 Conclusions

In this paper, an innovative approach for the synthesis of time-modulated arrays has been proposed. In order to reduce the power losses, a PSO -based optimization strategy has been adopted to minimize a closed-form relationship, which takes into account the whole sideband radiations in a direct way thus avoiding the computationally-expensive evaluation of the infinite set of harmonic patterns. Thanks to these key-features, the proposed technique represents an improvement with respect to state-of-the-art methods in terms of simplicity and efficiency as shown by some representative results.

Further investigations will concern with the extension of the PSO -based strategy to the synthesis of real-time adaptive systems suitable for communications as well as for the suppression of jamming signals.

References

- [1] H. E. Shanks and R. W. Bickmore, "Four-dimensional electromagnetic radiators," *Canad. J. Phys.*, vol. 37, pp. 263-275, Mar. 1959.
- [2] W. H. Kummer, A. T. Villeneuve, T. S. Fong, and F. G. Terrio, "Ultra-low sidelobes from time-modulated arrays," *IEEE Trans. Antennas Propag.*, vol. 11, no. 6, pp. 633-639, Nov. 1963.
- [3] R. W. Bickmore, "Time versus space in antenna theory," in *Microwave Scanning Antennas*, R. C. Hansen, Ed. Los Altos, CA: Peninsula, 1985, vol. III, ch. 4.

- [4] J. C. Brégains, J. Fondevila, G. Franceschetti, and F. Ares, "Signal radiation and power losses of time-modulated arrays," *IEEE Trans. Antennas Propag.*, vol. 56, no. 6, pp. 1799-1804, Jun. 2008.
- [5] S. Yang, Y. B. Gan, A. Qing, and P. K. Tan, "Design of a uniform amplitude time modulated linear array with optimized time sequences," *IEEE Trans. Antennas Propag.*, vol. 53, no. 7, pp. 2337-2339, Jul. 2005.
- [6] A. Tennant and B. Chambers, "Time-switched array analysis of phase-switched screens," *IEEE Trans. Antennas Propag.*, vol. 57, no. 3, pp. 808-812, Mar. 2009 .
- [7] J. Fondevila, J. C. Brégains, F. Ares, and E. Moreno, "Application of time modulation in the synthesis of sum and difference patterns by using linear arrays," *Microw. Opt. Technol. Lett.*, vol. 48, pp. 829-832, 2006.
- [8] S. Yang, Y. B. Gan, and A. Qing, "Sideband suppression in time-modulated linear arrays by the differential evolution algorithm," *IEEE Antennas Wireless Propag. Lett.*, vol. 1, pp. 173-175, 2002.
- [9] S. Yang, Y. B. Gan, and P. K. Tan, "A new technique for power-pattern synthesis in time-modulated linear arrays," *IEEE Antennas Wireless Propag. Lett.*, vol. 2, pp. 285-287, 2003.
- [10] J. Fondevila, J. C. Brégains, F. Ares, and E. Moreno, "Optimizing uniformly excited linear arrays through time modulation," *IEEE Antennas Wireless Propag. Lett.*, vol. 3, pp. 298-301, 2004.
- [11] J. Kennedy, R. C. Eberhart, and Y. Shi, *Swarm Intelligence*. San Francisco, CA: Morgan Kaufmann, 2001.
- [12] S. Yang, Y. B. Gan, and P. K. Tan, "Evaluation of directivity and gain for time-modulated linear antenna arrays," *Microw. Opt. Technol. Lett.*, vol. 42, no. 2, pp. 167-171, Jul. 2004.
- [13] C. L. Dolph, "A current distribution for broadside arrays which optimizes the relationship between beam width and sidelobe level," *Proc. IRE*, vol. 34, pp. 335-348, 1946.

FIGURE CAPTIONS

- **Figure 1.** *SR Minimization* ($N = 30, d = 0.7\lambda$) - Switch-on time sequence synthesized with the *PSO*-based approach.
- **Figure 2.** *SR Minimization* ($N = 30, d = 0.7\lambda$) - Normalized power patterns at the carrier frequency ($h = 0$) and related to the sideband radiations ($h = 1, 2$) in correspondence with the pulse sequence in Fig. 1.
- **Figure 3.** *SR Minimization* ($N = 30, d = 0.7\lambda$) - Behavior of the cost function and its terms during the iterative *PSO*-based minimization.
- **Figure 4.** *SR Minimization* ($N = 30, d = 0.7\lambda$) - Behavior of the sideband levels $SBL^{(h)}$ when $h \in [0, 30]$. Reference [10] and values computed with the *PSO*-optimized pulse sequence in Fig.2.
- **Figure 5.** *Performance Analysis* ($N = 30, d = 0.7\lambda$) - Behavior of the power losses \mathcal{P}^{SR} and directivity D^T versus the *SLL* for Dolph-Chebyshev patterns [13].

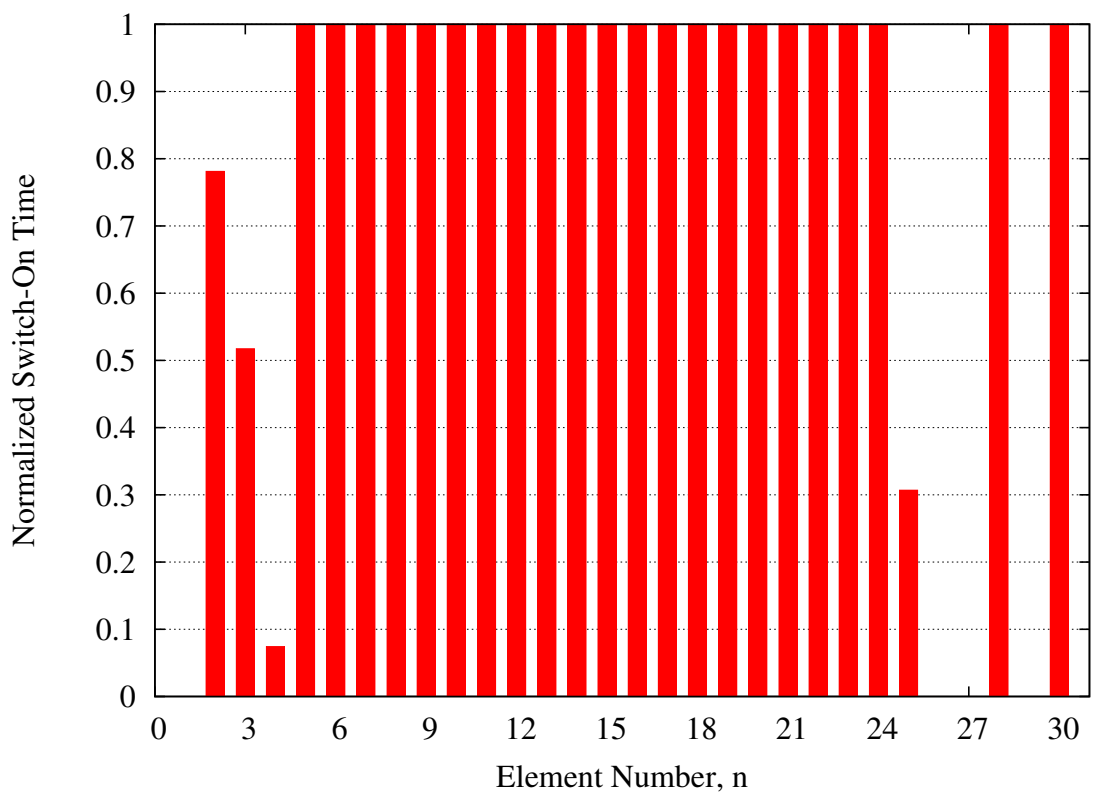


Fig. 1 - L. Poli *et al.*, “Handling sideband radiations in time-modulated arrays ...”

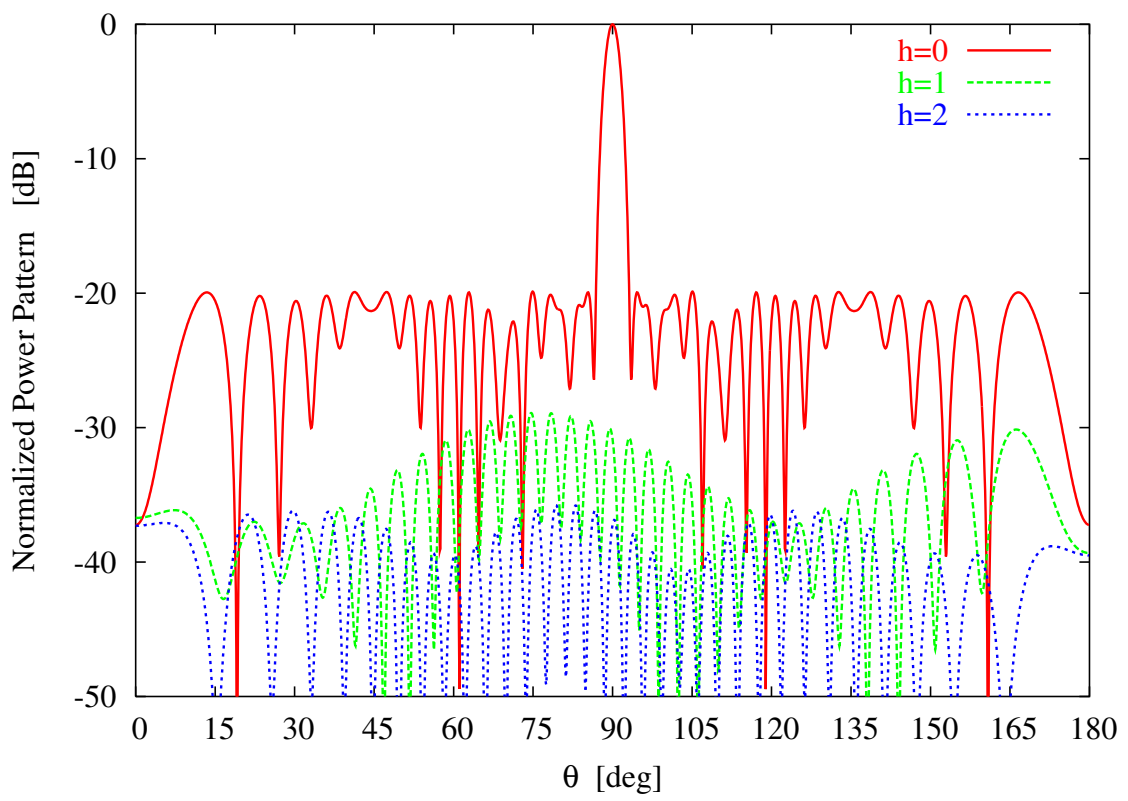


Fig. 2 - L. Poli *et al.*, “Handling sideband radiations in time-modulated arrays ...”

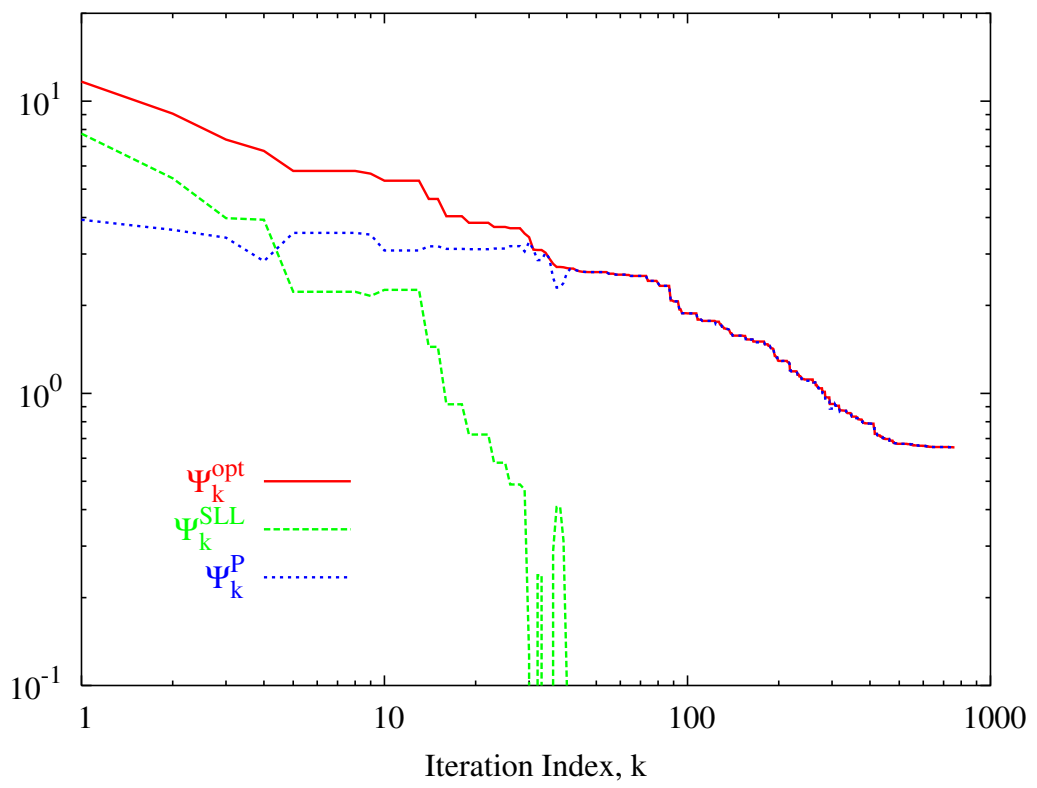


Fig. 3 - L. Poli *et al.*, “Handling sideband radiations in time-modulated arrays ...”

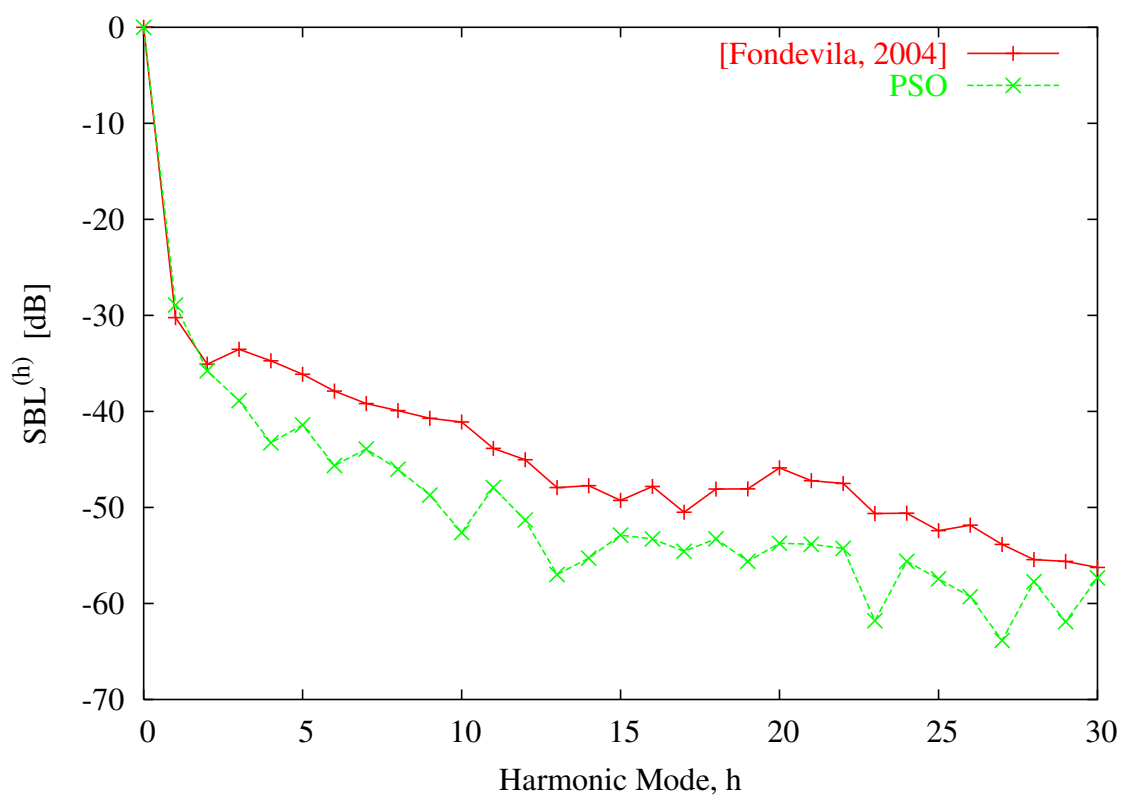


Fig. 4 - L. Poli *et al.*, “Handling sideband radiations in time-modulated arrays ...”

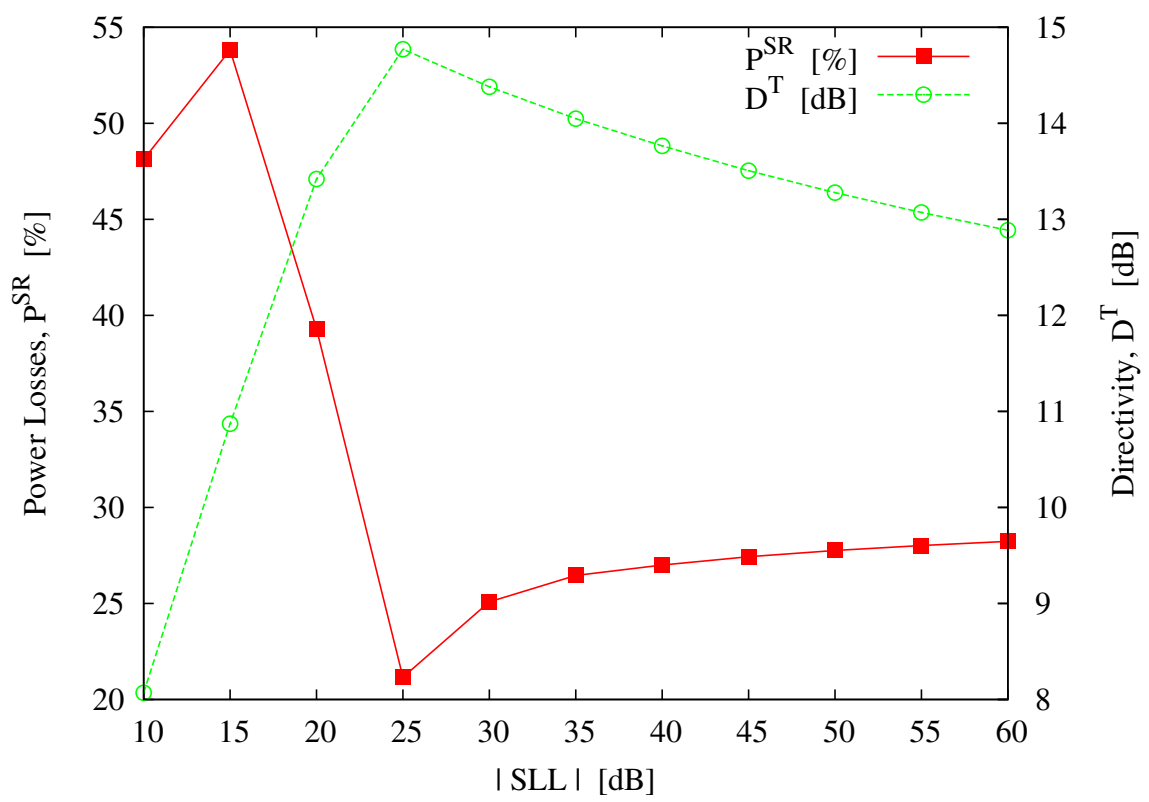


Fig. 5 - L. Poli *et al.*, “Handling sideband radiations in time-modulated arrays ...”